

GAMBE: Thermal Neutron Detection System Based on a Sandwich Configuration of Silicon Semiconductor Detector Coupled with Neutron Reactive Material

A. Ahmed^{a,b,*}, S. Burdin^{a,*}, G. Casse^a, H. van Zalinge^b, S. Powel^a, J. Rees^a, A. Smith^a, I. Tsurin^a

^aUniversity of Liverpool, Department of Physics, Liverpool, UK, L69 7ZE

^bUniversity of Liverpool, Department of Electrical Engineering and Electronics, Liverpool, UK, L69 3GJ

Abstract

Silicon semiconductor detectors are used efficiently for neutron detection when coated with a suitable material. They detect secondary reaction products resulting from the interaction of thermal neutrons with a neutron sensitive material such as ${}^6\text{LiF}$. In the present work, the efficiency of the thermal neutron detector system, GAMBE, is discussed. This detector system based on two silicon sensors of 1 cm^2 active area and a layer of ${}^6\text{LiF}$ (1.5 ± 0.6) mg/cm^2 thick in a sandwich configuration. This arrangement achieves total and coincidence detection efficiency of $(4.1 \pm 0.5)\%$ and $(0.9 \pm 0.3)\%$ respectively. The coincidence method defines a true neutron hit by the simultaneous signal recorded by the two sensors facing the conversion film. This coincidence methodology is applied to enhance the rejection factor of fake hits due to high gamma background conditions up to 10^8 as discussed in previous work. Geant simulation indicates that total and coincidence detection efficiency up to 55% and 18% are possible using an advanced design of stacked detectors.

Keywords: neutron detector, semiconductor detector, coated semiconductor detector, neutron detection, neutron conversion.

1. Introduction

Detection of thermal neutrons is a fundamental topic in many areas of nuclear science. It is used for varying applications such as reactor instrumentation, special nuclear material detection (SNM) [1], particle physics, material science [2] and radiation safety [3]. However, neutrons are neutral particles which cannot interact with matter by means of Coulomb force, which forms an energy loss mechanism for charged particles and electrons. Also, neutrons can travel through many centimeters of matter without any interaction and thus, can be totally unseen by a conventional detector [4]. Therefore, there are different types of materials which are used as a converter for thermal neutrons, which usually are in thermodynamic equilibrium with the surrounding medium and their most probable energy at a room temperature of 290 K is 0.025 eV. These neutrons interact with the nucleus of these conversion materials and as a result, the neutron may produce secondary radiation, or the energy and direction of this neutron change significantly. Secondary radiation arising from these neutrons interactions are mainly heavy charged particles. These particles can be produced by neutron-induced nuclear reactions, or they may result from the nuclei of the absorbing material itself, which gain enough energy from an eventual collision with a neutron. Consequently, the detection of thermal neutrons depends on this secondary radiation, and most neutron detectors utilise some materials with a large absorption cross section for a high detection efficiency. Moreover, the reaction products must have the capability to leave the

material with positive detection energies [5, 6]. The three most often studied neutron reactive materials for such a detector are ${}^6\text{Li}$, ${}^{10}\text{B}$, or natural ${}^{157}\text{Gd}$ [7].

${}^6\text{Li}$ has a thermal neutron absorption cross section (σ) of 900 b, which decreases by increasing neutron energy [5]. The primary reaction of neutron interactions with ${}^6\text{Li}$ is ${}^6\text{Li}(n,\alpha){}^3\text{H}$; this reaction produces an alpha particle (at 2.05 MeV) and a triton (at 2.73 MeV) in opposite directions with total Q-value of 4.78 MeV. Although ${}^6\text{Li}$ has a smaller thermal neutron absorption cross section than ${}^{10}\text{B}$ and ${}^{157}\text{Gd}$, the higher energy reaction products make it attractive for thermal neutron detection. Furthermore, the low atomic density and the low mass density of ${}^6\text{Li}$ result in a large reaction product range exceeding the ranges of the reaction products for ${}^{10}\text{B}$ film, with a sufficient range for triton $L_H = 126.77\ \mu\text{m}$ and an efficient range for alpha $L_\alpha = 19.05\ \mu\text{m}$. ${}^6\text{Li}$ could be used in the pure form as a neutron reactive material although it demands cumbersome handling procedures because of its corrosiveness and chemical reactivity. Due to this chemical reactivity of pure ${}^6\text{Li}$, it could alternatively be used in the form of ${}^6\text{LiF}$, which is more stable, however, the range of reaction products will be affected with $L_H = 29.25\ \mu\text{m}$ and $L_\alpha = 4.64\ \mu\text{m}$ [8].

Coated semiconductor diodes such as silicon with a thin film of neutron reactive material have been discussed for decades as neutron detectors [9]. Neutrons interacting in the reactive layer cause the spontaneous ejection of the secondary reaction products entering the adjacent semiconductor detector. This secondary radiation creates numerous electron-hole pairs whose charge can be measured through a shaped voltage pulse. These sensors offer valuable features, such as low weight, bias voltage, battery consumption and a high count rate capability [10]. The high density of the semiconductor allows an optimum de-

*Corresponding authors

Email addresses: m.o.ahmed@liv.ac.uk (A. Ahmed), s.burdin@liv.ac.uk (S. Burdin)

60 tector compactness, because of the short ranges of the reaction
 61 products. That suggests silicon as a best choice for thermal-
 62 neutron detector also because of the relatively low atomic num-
 63 ber of silicon ($Z = 14$), which decreases gamma-ray interac-
 64 tion probability [11]. In fact, the sensitivity to gamma radi-
 65 ation is expected to be low in Si wafer for a thickness range-
 66 of 30–300 μm . For instance, Si sensors of 300 μm thick has-
 67 gamma-ray detection efficiency up to 100% for gamma photons-
 68 of 10 keV, falling approximately to 1% for 150 keV [12].

69 In this work, the feasibility of using enriched ${}^6\text{Li}$ with sil-
 70 icon sensors in a sandwich configuration as a thermal neutron-
 71 counter, called GAMBE, has been investigated. Tests have been-
 72 performed using ${}^6\text{Li}$ in the form of ${}^6\text{LiF}$ coating film which-
 73 was applied to a silicon semiconductor radiation sensor where-
 74 the reaction products will be measured. The basic design con-
 75 sideration was studied using Geant4 simulations to identify the-
 76 optimal thickness of ${}^6\text{LiF}$ film, which was capable of achiev-
 77 ing the highest total and coincidence detection efficiency. In-
 78 addition, experimental measurements were carried out using an-
 79 ${}^{241}\text{Am}$ - ${}^9\text{Be}$ neutron source with the detector placed in a partic-
 80 ular position 75 cm away from the neutron source. Thus, the
 81 thermal neutron flux and the GAMBE detection efficiency were
 82 determined at this position as presented. Finally, it has been
 83 suggested that using an advanced configuration of a stacked de-
 84 tector will improve the whole GAMBE performance.

85 2. Geant4 modelling approach

86 Geant4 is a toolkit for simulating the passage of particles
 87 through matter. It includes a complete range of functionality
 88 such as tracking, geometry, physics models, and hits. It has
 89 been created exploiting software engineering, object-oriented
 90 technology and implemented in the C++ programming lan-
 91 guage. It has been used for a variety of applications in particle
 92 physics, nuclear physics, accelerator design, space engineering,
 93 and medical physics [13].

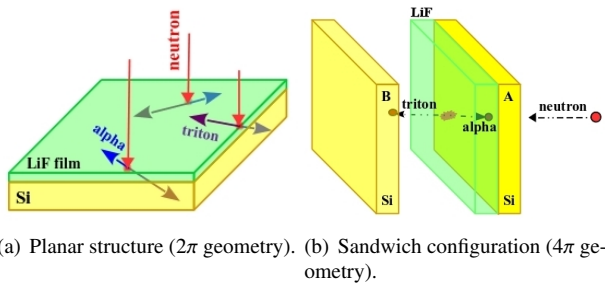


Figure 1: Principle of neutron detection using a) planar Si semiconductor
 coated with ${}^6\text{LiF}$ film b) GAMBE, thermal neutron detector.

94 Planar design is the most straight forward adaptation of semi-
 95 conductor detector for neutron detection. However, it has its
 96 limitation. Firstly, the neutron capture probability in the con-
 97 verter is increasing with increasing the converter layer thick-
 98 ness in one hand, but on the other hand, the chance that the
 99 neutron capture reaction products will reach the detector sen-
 100 sitive part may be severely reduced with the growing of this
 101 converter layer. Therefore, an optimal converter thickness of

${}^6\text{LiF}$ material has to be found. Secondly, only those charged
 particles which are ejected in the direction of diode interface
 would be detected. This is known as 2π geometry as presented
 in fig. 1(a) allowing only up to half of the primary reaction
 products to generate e–h pairs inside the depletion region of
 semiconductor material. Hence, sandwich stacking as shown in
 fig. 1(b) will lead to 4π collection of primary reaction products;
 as the detection of either alpha or triton becomes possible and
 this increases the detection efficiency.

Simulations have been performed using Geant4 to identify
 the optimal ${}^6\text{LiF}$ film thickness where neutron detection effi-
 ciency is the highest using a sandwich configuration of two sili-
 con detectors. The sandwich detector geometry consists of two
 $12.5 \times 12.5 \text{ mm}^2$ silicon diodes which are assigned as A and B
 with a thickness of 300 μm . The sensitive ${}^6\text{LiF}$ film with an ad-
 justable thickness is located between the two Si sensors where
 it adheres to sensor A and the two sensors are separated by a
 300 μm gap (see fig. 1(b)). There is also a 100 nm Al contact
 covering the active region of both silicon sensors.

For the simulation, each event begins with the generation of a
 random position within the sensitive film volume where a ther-
 mal neutron will be captured. From this point, one alpha is
 assigned an arbitrary direction with an energy of 2.05 MeV
 and a triton is assigned the opposite direction with an energy
 of 2.73 MeV. This model assumes that neutron capture is dis-
 tributed uniformly within the converter film. This is a good
 approximation for the thickness range under investigation be-
 cause the probability of a thermal neutron absorption would be
 constant over the entire volume of the converter film. For each
 event (alpha or triton), the energy deposited in each of the two
 silicon sensors is computed.

In this simulation the thermal neutron detection efficiency, ε ,
 is calculated by [6]

$$\varepsilon = \frac{n}{N} \times P(x) = \frac{n}{N} \times \{1 - \exp(-\frac{N_A}{w_A} \times \rho \times \sigma \times x)\} \quad (1)$$

where $\frac{n}{N}$ is the ratio of the detected charged particles (n) by Si
 detector to the number of generated neutrons (N) within the
 film. $P(x)$ is the probability of an incident thermal neutron
 being captured as a function of the reactive film thickness, x .
 N_A is Avogadro's number, w_A the atomic or molecular weight
 of the reactive film, ρ the density of the reactive film and σ
 the thermal-neutron cross-section, for ${}^6\text{Li}$ 940 b. A neutron is
 counted by detecting either alpha or triton as a single or/and a
 coincident event, this is defined as total detection efficiency of
 the detector (ε_t). Detecting neutron capture products in coinci-
 dence is a method based on detection both of reaction products
 (alpha and triton) by two Si sensors at the same time and, thus,
 the coincidence detection efficiency (ε_c) of the detector is de-
 fined.

The simulated thermal neutron detection efficiency for a
 range of ${}^6\text{LiF}$ film thicknesses is displayed in fig. 2 which shows
 the effect of ${}^6\text{LiF}$ film thickness increment on both total and co-
 incidence detection efficiencies. Since, the detection efficiency
 depends on both the probability that neutron to be captured and
 the chance that secondary particles born in the ${}^6\text{LiF}$ film will
 be capable of reaching the sensitive detector volume. The total

157 and coincidence detection efficiencies increase up to a certain
 158 value of a ${}^6\text{LiF}$ film thickness then they will decrease. Results
 159 indicate that the optimal film thicknesses for the highest total
 160 and coincidence detection efficiencies of 7.5 and 1.1% are 8.14
 161 and 1.16 mg/cm^2 respectively.

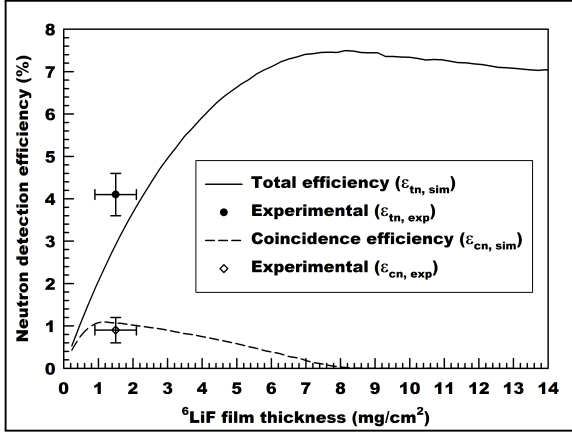


Figure 2: Variation of thermal neutron detection efficiency as a function of ${}^6\text{LiF}$ film thickness.

3. Experimental work

162
 163 A 6 mol/l ${}^6\text{LiF}$ solution was prepared by dissolving 3 g of
 164 ball milled ${}^6\text{LiF}$ powder (Sigma-Aldrich 95% enriched ${}^6\text{Li}$) in
 165 20 cc ethanol. The ${}^6\text{LiF}$ solution was mixed with a ratio of
 166 1:1 with a solution of 1 w/v% polyvinylpyrrolidone (Sigma-
 167 Aldrich PVP, MW 700000) in ethanol with a molar concentra-
 168 tion of 1.43×10^{-4} mol/l, which is used as an adhesive materi-
 169 al. This mixture of ${}^6\text{LiF}/\text{PVP}$ was precipitated on the surface
 170 of the Si sensor (total area of $1.25 \times 1.25 \text{ cm}^2$). The mass of
 171 ${}^6\text{LiF}/\text{PVP}$ solution to be poured on Si sensor substrate is esti-
 172 mated as a function of the required ${}^6\text{LiF}$ film thickness. The
 173 mass of the poured solution was measured with a scale, where
 174 (2.4 ± 0.1) mg of the mixture was applied to the Si sensor to
 175 cover the whole surface area of $1.25 \times 1.25 \text{ cm}^2$. This precip-
 176 itated mixture was dried at room temperature to avoid cracks
 177 and to form a uniform film over the area of Si substrate. In or-
 178 der to characterise the surface roughness of the deposited film,
 179 an Atomic Force Microscope (AFM) and a scanning Keyence
 180 VHX5000 Digital Microscope (KVDM) were used. It was
 181 found that the precipitated ${}^6\text{LiF}$ film on the silicon sensor is not
 182 uniformly distributed and has a surface roughness of $2.5 \mu\text{m}$.
 183 This results in an error in the mass distribution of $\pm 0.6 \text{ mg}/\text{cm}^2$
 184 over the whole area of the formed ${}^6\text{LiF}$ film, which can be con-
 185 sidered as a reason for the variation of the detection efficiency.
 186 Consequently, the determined thickness of the precipitated ${}^6\text{LiF}$
 187 film is $(1.5 \pm 0.6) \text{ mg}/\text{cm}^2$.

188 Experimental measurements have been carried out using
 189 sandwich detector configuration with and without neutron con-
 190 verter material, in order to differentiate between neutron and
 191 gamma-ray events. ${}^6\text{LiF}$ film $(1.5 \pm 0.6) \text{ mg}/\text{cm}^2$ thick has been
 192 used as a neutron converter in this sandwich configuration (see
 193 fig. 1(b)). In each measurement, the whole GAMBE assembly
 194 was oriented in such a manner that coated Si diode sensor A was

back irradiated by thermal neutrons whereas sensor B was fac-
 ing them. The entire sensor-converter system was mounted in
 an aluminium box designed to eliminate photoelectric noise as
 well as to decrease the effect of gamma-ray background. The
 detector has been placed in a particular position in front of a
 1 Ci ${}^{241}\text{Am}-{}^9\text{Be}$ neutron source, where neutrons are emitted as
 part of the reaction $\text{Be}(\alpha, n)\text{C}^*$.

Thermal neutron flux has been measured using the ${}^3\text{He}$ de-
 tector tube as can be seen in fig. 3. The tube is 50 cm away
 from the end of the neutron tank, and the 1 Ci ${}^{241}\text{Am}-{}^9\text{Be}$ neu-
 tron source is 25 cm inside the water tank. This position is
 referred as the calibration position. The ${}^3\text{He}$ detector tube is an
 industry standard 2 in. (5 cm) diameter, 36 in. (90 cm), active
 length, filled to a pressure of 2 atm, and operating at a high volt-
 age of 1100 V. Its typical thermal neutron detection efficiency
 is $> 60\%$. Furthermore, the neutron sensitivity of these detec-
 tors is 236 cps/nv (nv is thermal neutron flux, neutrons/ cm^2/s).
 Approximately 3 cps/nv per cm active tube length assuming no
 degradation of performance over the lifetime of the detector.

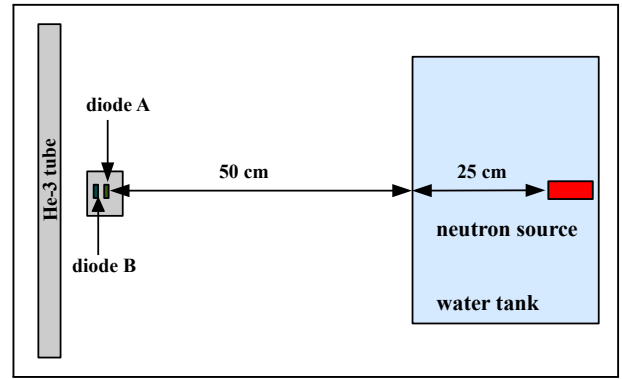


Figure 3: Experimental layout where the detector is at the calibration position.

Another detector such as the NMS017NG3 neutron survey
 monitor has been used to characterise the variation in the neu-
 tron flux along the length of the ${}^3\text{He}$ detector tube. This detector
 has demonstrated that the neutron flux at the center of the ${}^3\text{He}$
 detector tube is 1.40 times greater than over the entire length of
 the ${}^3\text{He}$ detector tube.

4. Results and Discussion

4.1. Thermal neutron flux

Thermal neutron flux has been determined at the cali-
 bration position corresponding to a detection rate of
 (1013.01 ± 0.07) cps by ${}^3\text{He}$ thermal neutron detector. As a re-
 sult, the determined neutron flux is 6 nv ($\text{n}/\text{s}/\text{cm}^2$). It is this
 figure that has been used to calculate the total and coincidence
 detection efficiency of the thermal neutron detector.

4.2. GAMBE detection efficiency

The detection efficiency has been determined by integrating
 the area under the curve for both total and coincidence events
 and then dividing the results by the neutron flux ($\text{n}/\text{cm}^2/\text{s}$)
 through the converter film. All events belonging to gamma-
 ray interaction with the sandwich detector of bare silicon sen-
 sors, either they are single or coincidence events have been sub-
 tracted from the obtained energy spectrum as presented in fig. 4.

236 This subtraction affects the count rate especially at lower energy²⁷¹
 237 range where there is a possibility of a combination between α -²⁷²
 238 particle and γ -ray interaction with silicon detector. However,²⁷³
 239 this step insures that the evaluated detection efficiency is an ab-²⁷⁴
 240 solute thermal neutron detection efficiency.

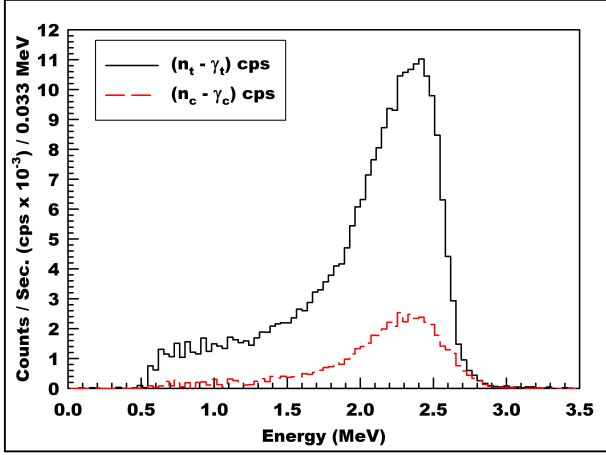


Figure 4: Spectra of energy deposited in both Si sensors of the detector as a function of a ⁶LiF film (1.5 ± 0.6) mg/cm² thick.

241 Results show that ⁶LiF film of (1.5 ± 0.6) mg/cm² thick in
 242 a sandwich detector configuration can achieve total and coinci-
 243 dence detection efficiency of (4.1 ± 0.5)% and (0.9 ± 0.3)%
 244 respectively. The results are compatible and in agreement with
 245 the theoretical investigation as displayed and compared in fig. 2,
 246 where the variation of the surface roughness of the converter
 247 film has been taken into consideration. Although, the coinci-
 248 dence detection methodology affects and decreases the detection
 249 efficiency of, GAMBE, thermal neutron detection system,
 250 It provides a very good method for rejecting the spurious hits
 251 coming from gamma photons, which are usually present in the
 252 neutron field under measurement.

253 5. Neutron detection efficiency enhancement

254 A method has been proposed to improve the thermal neutron
 255 detection efficiency by using a stacked detector configuration.
 256 The concept of this method was based on eq. (1) by introducing
 257 a new factor m in the probability of thermal neutron absorption
 258 $P(x)$. Where m represents the number of detectors of sandwich
 259 configuration with a converter material in the stack as depicted
 260 in eq. (2).

$$261 \quad \varepsilon = \frac{n}{N} \times P(x) = \frac{n}{N} \times \left\{ 1 - \exp\left(-\frac{N_A}{w_A} \times \rho \times \sigma \times x \times m\right) \right\} \quad (2)$$

262 Hence, the purpose of multi-layers approach is to increase the
 263 thermal neutron detection efficiency by increasing the active
 264 area where the neutron could be captured. However, The detec-
 265 tion efficiency is not expected to scale linearly with increasing
 266 the number of stacked detectors. This is because the initial neu-
 267 tron flux will be attenuated by each of the neutron sensitive ⁶LiF
 268 film and as a result, the neutron flux decreases for each subse-
 269 quent detector. Moreover, in each reactive layer a proportion of
 270 incident neutrons are captured and not all result in a detected

event. It should be pointed out that the rate of increment in the
 detection efficiency reduces, as the number of detectors in the
 stack increases.

275 From the modelling, it is expected that a multiple-layer pro-
 276 posal of 20 sandwich detectors can achieve total and coinci-
 277 dence detection efficiencies up to 55 and 18% respectively. The
 278 advanced stacked detectors design not only affects the detection
 279 efficiency but it also influences the optimum ⁶LiF film thick-
 280 ness for a particular number of sandwich detectors in the stack.
 281 It is found that the optimum thickness for the individual ⁶LiF
 282 neutron reactive films decreases as the number of detectors in
 283 the multiple layers configuration increases. The results of this
 284 study also indicate that for a specific number of sandwich de-
 285 tector there is an ideal thickness of ⁶LiF film that maximises
 286 the total and coincidence detection efficiencies as displayed in
 287 figs. 5 and 6 respectively. In addition, figs. 5 and 6 illustrate
 288 that the range of ⁶LiF thickness is dependent on which type of
 289 the detection efficiency will be used for neutron identification.
 290 Finally, the overall device design should incorporate a reason-
 291 able number of detectors compatible with the available power
 supply and output electronics.

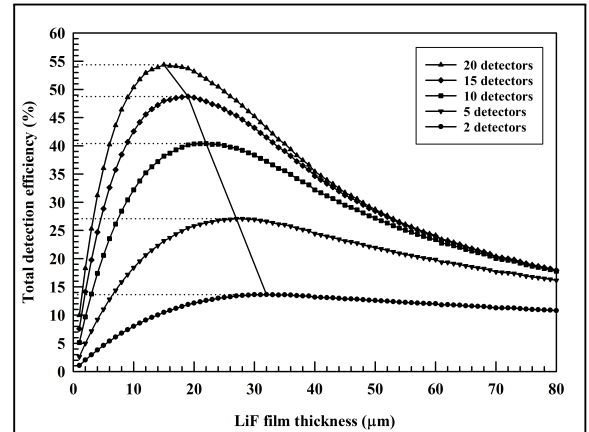


Figure 5: Total detection efficiency as a function of enriched ⁶LiF film thickness and number of layers.

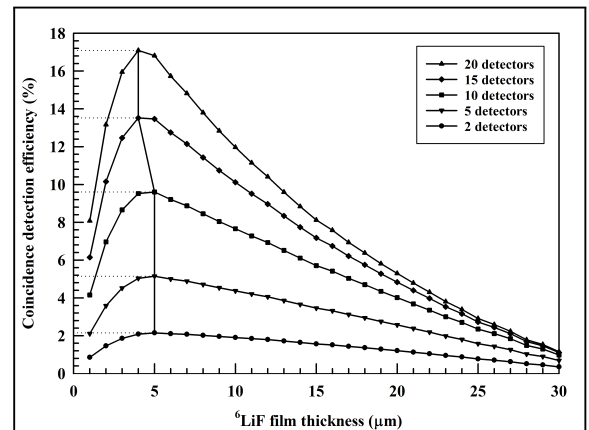


Figure 6: Coincidence detection efficiency as a function of enriched ⁶LiF film thickness and number of layers.

6. Conclusion

The aim of the present research was to examine the practicality of using enriched ${}^6\text{Li}$ as a ${}^6\text{LiF}$ film with silicon sensors around 1 cm^2 active area in a sandwich configuration as a thermal neutron detector. The expected efficiency for this sandwich style has been described as a function of ${}^6\text{LiF}$ converter film thickness. For instance, the sandwich configuration allows for optimised total and coincidence detection efficiencies of 7.5 and 1.1% corresponding to ${}^6\text{LiF}$ film of 8.14 and 1.16 mg/cm^2 respectively. Tests have been performed using ${}^6\text{LiF}$ film of $(1.5 \pm 0.6)\text{ mg/cm}^2$ thick to examine the coincidence detection efficiency which will be capable of enhancing gamma-ray rejection factor. The detector was capable of achieving total and coincidence detection efficiencies of $(4.1 \pm 0.5)\%$ and $(0.9 \pm 0.3)\%$ respectively. In addition, if the detector stacking technique is used, dramatic increases in thermal neutron detection efficiency can occur. For instance, stacking 20 individual sandwich detectors can increase the total and coincidence detection efficiencies up to 55% and 18% which are comparable to the detection efficiency of ${}^3\text{He}$ detector tubes. Hence, the future work will focus on building the neutron detection system, GAMBE, which has a multilayer configuration in order to validate the theoretical study and to investigate the behaviour of the stacked detector with the background gamma radiation.

References

- [1] K. A. Jordan, T. Gozani, Detection of 235 u in hydrogenous cargo with differential die-away analysis and optimized neutron detectors, Nuclear Instruments and Methods in Physics Research Section A: Accelerators, Spectrometers, Detectors and Associated Equipment 579 (1) (2007) 388–390.
- [2] A. Szytuła, Neutron scattering for materials science, in: Solid State Phenomena, Vol. 112, Trans Tech Publ, 2006, pp. 39–60.
- [3] E. B. Podgoršak, Radiation physics for medical physicists, Springer, 2006.
- [4] A. N. Caruso, The physics of solid-state neutron detector materials and geometries, Journal of Physics: Condensed Matter 22 (44) (2010) 443201.
- [5] G. F. Knoll, Radiation detection and measurement, John Wiley & Sons, 2010.
- [6] C. Leroy, P.-G. Rancoita, Principles of radiation interaction in matter and detection, Vol. 2, World Scientific, 2009.
- [7] D. S. McGregor, M. Hammig, Y.-H. Yang, H. Gersch, R. Klann, Design considerations for thin film coated semiconductor thermal neutron detectors: basics regarding alpha particle emitting neutron reactive films, Nuclear Instruments and Methods in Physics Research Section A: Accelerators, Spectrometers, Detectors and Associated Equipment 500 (1) (2003) 272–308.
- [8] D. S. McGregor, R. T. Klann, H. K. Gersch, J. D. Sanders, Designs for thin-film-coated semiconductor thermal neutron detectors, in: Nuclear Science Symposium Conference Record (2001 IEEE), Vol. 4, 2001, pp. 2454–2458.
- [9] D. S. McGregor, H. K. Gersch, J. D. Sanders, R. T. Klann, J. T. Lindsay, Thin-film-coated detectors for neutron detection, Journal of the Korean Association for Radiation Protection 26 (2001) 167–175.
- [10] G. Lutz, et al., Semiconductor radiation detectors, Vol. 10, Springer, 1999.
- [11] C. Guardiola, C. Fleta, G. Pellegrini, F. García, D. Quirion, J. Rodríguez, M. Lozano, Ultra-thin 3d silicon sensors for neutron detection, Journal of Instrumentation 7 (03) (2012) P03006.
- [12] C. Petrillo, F. Sacchetti, O. Toker, N. Rhodes, Solid state neutron detectors, Nuclear Instruments and Methods in Physics Research Section A: Accelerators, Spectrometers, Detectors and Associated Equipment 378 (3) (1996) 541–551.
- [13] S. Agostinelli, J. Allison, K. a. Amako, J. Apostolakis, H. Araujo, P. Arce, M. Asai, D. Axen, S. Banerjee, G. Barrand, et al., Geant4a simulation toolkit, Nuclear instruments and methods in physics research section A: Accelerators, Spectrometers, Detectors and Associated Equipment 506 (3) (2003) 250–303.